

Toward grid-interactive and low-carbon buildings: A comparative analysis of artificial intelligence-driven optimization of renewable sizing and demand-side control

Karim ElNaggar^{1*}, Rana Maher¹ Motaz Amer², and Amany El-Zonkoly¹

¹Electrical & Control Engineering Department, College of Engineering and Technology, Arab Academy for Science, Technology & Maritime Transport, Alexandria, Egypt

²Basic and Applied Sciences Institute, College of Engineering and Technology, Arab Academy for Science, Technology & Maritime Transport, Alexandria, Egypt
karimelnaggar726@yahoo.com, rana-maher@aast.edu, motaz.amer@aast.edu, amanyelz@yahoo.com

ARTICLE INFO

Article History:

Received: November 11, 2025

Revised: November 25, 2025

Accepted: November 27, 2025

Published online: January 6, 2026

Keywords:

Building energy management system

Demand-side management

Photovoltaic sizing

Reinforcement learning

AMS Classification 2010:

76M12; 76R10; 80A20; 76D05; 65N30

ABSTRACT

As buildings account for nearly one-third of global energy consumption, improving their energy performance and renewable integration is essential for achieving sustainability targets. Traditional building energy management systems (BEMS), often rule-based and static, struggle to adapt to fluctuating demands, variable tariffs, and the intermittency of solar resources. This study introduces an integrated, artificial intelligence (AI)-driven BEMS framework that jointly optimizes rooftop photovoltaic (PV) sizing and adaptive demand-side management (DSM) using reinforcement learning (Q-Learning) and benchmarks its performance against two established deterministic tools: HOMER Pro for techno-economic PV sizing and particle swarm optimization (PSO) for DSM load scheduling. Using realistic hourly building loads, meteorological data, and time-of-use pricing, the Q-Learning model converged to a PV-inverter configuration closely aligned with HOMER Pro's optimum, achieving a slightly lower net present cost (−1.85%) and a modest increase in renewable fraction (+3.1%). In DSM applications, Q-Learning consistently outperformed PSO by shifting a larger share of flexible loads and securing higher daily cost reductions. Under grid-only conditions, Q-Learning reduced energy costs by 7.58% in winter and 8.27% in summer, while PV-integrated scenarios achieved savings of 35.14% and 26.89%, respectively. These results demonstrate that reinforcement learning can effectively enhance the performance of conventional BEMS approaches by providing more adaptive scheduling aligned with tariff structures and solar availability. The proposed framework supports more efficient, flexible, and sustainable building operations, highlighting the practical potential of AI-driven energy management in modern grid-interactive environments.



1. Introduction

Buildings account for nearly one-third of global energy consumption, making them a critical focus in the pursuit of carbon neutrality and sustainable

energy transitions. Despite the increasing integration of renewable energy sources, traditional building energy management systems (BEMS), typically rule-based and static, struggle to respond to fluctuating demand, occupant variability, and renewable generation uncertainty. These

*Corresponding Author

limitations reduce their ability to adapt in real time and to optimize operational efficiency.

Artificial intelligence (AI) offers promising solutions to these challenges. AI-driven BEMS apply data-driven techniques such as machine learning and predictive analytics to monitor, forecast, and optimize building energy use. These systems enable real-time demand-side management (DSM), allowing energy consumption to be adjusted in response to supply conditions or dynamic pricing, and they also improve the sizing and operation of photovoltaic–battery storage systems (PV-storage). Recent studies have shown their potential in reducing peak loads, enhancing occupant comfort, and improving system responsiveness.^{1,2}

However, there are important concerns about the interpretability, cost, and scalability of these systems in real-world applications.³ Moreover, most existing approaches address either DSM or PV-storage optimization in isolation, lacking a unified framework that integrates both functions in a scalable, adaptive manner.^{4,5}

This study investigates whether AI-based control models can outperform conventional rule-based systems in managing DSM and optimizing PV-storage configurations. We propose a scalable, integrated BEMS framework and evaluate its performance using simulation tools such as HOMER Pro and MATLAB. Preliminary simulations showed measurable gains in load balancing and energy efficiency. This work is a step toward practical grid-interactive building energy systems.

The novelty of this work lies in the development of a unified, dual-layer AI-driven BEMS architecture in which reinforcement learning (RL) was applied both at the design stage (PV-inverter sizing) and at the operational stage (DSM scheduling) under identical boundary conditions. While RL has been applied to each problem independently, existing studies rarely evaluate both tasks within the same environment using consistent datasets, constraints, and performance metrics. This integrated formulation enables a direct and fair comparison between learning-based and deterministic tools and reveals interactions between sizing decisions and DSM behavior—an aspect largely overlooked in prior work.

2. Literature review

Recent research on BEMS highlights how the integration of AI, renewable energy resources,

and DSM has improved building energy performance. Modern systems rely on intelligent forecasting, adaptive control, and data-driven optimization to balance consumption, reduce operational costs, and improve occupant comfort. Studies confirm that AI-driven optimization enhances predictive control and fault detection, renewable integration transforms buildings into prosumers, and DSM strategies enable flexible, cost-efficient consumption.^{6,7} Cyber-physical energy systems and digital-twin architectures further enhance flexibility and resilience.⁸ Nevertheless, most frameworks still treat optimization, renewable integration, and DSM, separately. There remains a need for unified, intelligent BEMS models capable of coordinating these functions in real time for grid-interactive and occupant-centric operation.^{9,10}

2.1. Artificial intelligence/machine learning algorithms for optimization

Artificial intelligence and machine learning algorithms now form the core of advanced BEMS optimization, addressing nonlinear system dynamics and uncertainty. RL, especially Q-Learning and deep variants, enables adaptive, model-free control of energy scheduling. Deep Q-Learning and multi-agent RL architectures outperform classical optimization, achieving notable reductions in energy cost and discomfort.^{11–13} Hybrid RL–model predictive control (MPC) frameworks improve predictive stability, while swarm-based approaches such as particle swarm optimization (PSO) and quantum-enhanced PSO provide fast global convergence for renewable sizing and scheduling.^{14,15} Recent reviews emphasize that deep reinforcement learning (DRL) can outperform these heuristic and MPC-based methods by improving adaptability and learning efficiency in dynamic building environments.¹⁶

However, most results stem from simulation studies, and real-world deployments remain sparse due to modeling assumptions and system variability. **Table 1** shows that RL and PSO techniques have advanced optimization beyond static control. RL offers adaptability and long-term learning capability, while PSO ensures rapid global optimization for sizing and scheduling. Recent work combined RL’s learning ability with PSO’s fast convergence and MPC’s predictive control. The hybrid RL–MPC approach is particularly attractive, as it can respond effectively to uncertainty while respecting operational constraints.

Recent advancements in DRL, including Deep Q-Networks, Deep Deterministic Policy Gradient, and proximal policy optimization, have expanded the capability of learning-based controllers to operate in continuous action spaces while improving generalization in stochastic environments. Hybrid RL-MPC structures have also emerged as a promising direction, combining predictive forecasting with policy learning to enhance stability under uncertainty. These developments highlight the importance of benchmarking classical Q-Learning against more advanced RL techniques and position the present study within the broader research landscape of DRL-based BEMS optimization.

Despite these advances, scalability, interpretability, and computational efficiency remain open challenges, highlighting the need for explainable and resource-efficient AI frameworks for large-scale BEMS deployment.

2.2. Renewable energy sources in buildings

The integration of renewable energy sources within buildings has progressed rapidly, particularly through hybrid PV-wind-battery systems that enhance energy self-consumption and resilience. Techno-economic studies show that such configurations can meet up to 85% of annual load demand with leveled energy costs between 0.07 and 0.22 USD kW h⁻¹.^{20,21} Incorporating storage significantly improves reliability but introduces economic and control challenges, motivating exploration of hydrogen, gravity, and thermal storage options.^{22,23} Multi-source hybrids enhance flexibility by 30–40% and reduce carbon dioxide emissions by over 40%.^{24,25}

Hybrid renewable systems consistently outperform single-source designs in reliability, autonomy, and cost (see **Table 2**). The inclusion of diverse storage technologies enhances flexibility and emission reduction but increases control complexity. Regional economics and incentive structures heavily influence viability, particularly where low tariffs limit battery payback. Future research should prioritize AI-optimized hybrid controllers capable of dynamic coordination among PV, wind, and storage assets to maintain performance under variable grid and weather conditions.²⁵ Recent work also extends these optimization techniques to include electric vehicles and hybrid energy storage, highlighting new opportunities for integrated DSM-oriented energy management.²⁷

2.3. Demand-side management in buildings

Demand-side management enables active participation of buildings in balancing grid demand through intelligent control of loads and tariffs.²⁸ Traditional scheduling and rule-based control focused on reducing peak load and costs but lacked responsiveness to real-time occupancy and renewable variability.²⁹ Contemporary DSM integrates predictive analytics and AI-driven algorithms such as MPC, artificial neural networks, fuzzy logic, and hybrid optimization for adaptive and occupant-aware operation.^{30,31} Enhanced whale optimization and voltage optimization algorithms demonstrate superior load balancing, achieving up to 76% reduction in peak-to-average ratio and 23% cost savings.³²

Table 3 illustrates the shift from static scheduling to intelligent DSM frameworks. Recent models have achieved superior load flexibility, occupant comfort, and grid participation compared with traditional controls. Yet large-scale adoption remains constrained by interoperability, real-time computation, and privacy of behavioral data. Behavioral factors, such as comfort tolerance and override frequency, continue to challenge predictive accuracy in occupant-aware DSM. Future research should focus on unified, self-learning DSM architectures that seamlessly integrate with renewable generation and AI-based optimization to enable autonomous, grid-interactive BEMS operation.³³

3. Proposed model

This study presents an AI-driven BEMS integrating renewable energy sizing and adaptive DSM through reinforcement-learning-based optimization. The framework addresses two interrelated objectives as follows:

- (1) Determining the optimal rooftop PV generation capacity, and
- (2) Scheduling building loads adaptively to minimize operating cost and grid dependence.

For each objective, two independent optimization models were developed and executed within the same simulation environment: HOMER Pro and Q-Learning for renewable energy sizing, and PSO and Q-Learning for DSM. All four algorithms were implemented independently to enable a rigorous comparative analysis of algorithmic behavior, convergence, and performance under identical datasets and constraints. The case study focuses on a mid-rise apartment building modeled with hourly load data from the

Table 1. Comparative review of artificial intelligence/machine learning algorithms for building energy management systems optimization.

Study	Algorithm	Application	Key achievements	Limitation
Shen et al. ¹¹	Multi-agent deep RL	Building coordination	84% reduction in discomfort, 43% increase in renewable use	High complexity
Liu et al. ¹⁷	Deep Q-Learning	Home energy management	Lower cost than PSO models	Generalization issues
Ramesh et al. ¹²	Q-Learning, DQN, SARSA	Microgrid optimization	30% efficiency gain	Long training time
Ojand and Dagdougui ¹⁸	RL + MPC	Aggregator control	Improved cost reduction and peak management	Limited real-time integration
Menos-aikateriniadis et al. ¹⁴	PSO	Residential DSM	Fast convergence and simple implementation	Premature convergence
Gbadega and Sun ¹⁹	Constrained PSO-MPC	Storage optimization	Stable constraint handling 9.7% and 13.2% reduction in cost and emission, respectively	Computational overhead
Paul et al. ¹⁵	Quantum PSO	Grid-connected microgrids		High computational cost

Abbreviations: DQN: Deep Q-Networks; DSM: Demand-side management; MPC: Model predictive control; PSO: Particle swarm optimization; RL: Reinforcement learning; SARSA: State-action-reward-state-action.

Table 2. Representative hybrid renewable configurations in building applications.

Study	Configuration	Key findings	Limitations
Liu et al. ²⁰	PV–wind–battery	81% load coverage, LCOE 0.22 USD kW h ⁻¹	Storage validation limited
Das et al. ²¹	PV–wind–diesel–battery	45% CO ₂ cut, LCOE 0.07 USD kW h ⁻¹	Battery aging neglected
Chegari et al. ²⁴	PV–wind–pumped hydro–battery	39% self-sufficiency increase	Incomplete thermal model
Liu et al. ²⁰	PV–battery–EV (V2B)	+12% load coverage, –19% bill	EV degradation uncertainty
Emrani et al. ²²	PV–wind–gravity storage	35% lower storage requirement	Site-specific constraints
Jahanbin et al. ²⁶	PV–battery–hydrogen	+30% renewable fraction, –46% LCOE	Reduced hydrogen yield

Abbreviations: EV: Electric vehicle; LCOE: Levelized cost of energy; PV: Photovoltaic; USD: United States dollars.

United States (US) Department of Energy Reference Building Database,³⁷ meteorological data from NASA Prediction of Worldwide Energy Resources (POWER),³⁸ and real Miami time-of-use (ToU) electricity tariffs.³⁹ Two BEMS configurations were analyzed:

- (1) Grid-only BEMS: all electricity supplied from the utility grid; DSM aims to minimize daily cost.
- (2) Grid + PV BEMS: rooftop PV generation supplements grid supply; PV sizing precedes DSM scheduling.

Table 3. Representative demand-side management (DSM) approaches in buildings (2020–2025).

Study	Algorithm/method	Key contribution	Performance outcome
Hemanth et al. ²⁹	Grey Wolf optimization	Static load scheduling	15–20% cost cut
Farrokhifar et al. ³⁰	Model predictive control	Predictive multivariable DSM	Lower peak load
Philipo et al. ³⁴	ANN control	PV-battery microgrid DSM	31% peak reduction
Jasim et al. ³²	VOA/EWOA hybrid	Dynamic tariff optimization	23% cost saving, 76% PAR reduction
Tepe and Irmak ³¹	Fuzzy logic	Real-time pricing response	Improved comfort
Doma et al. ³⁵	Occupancy model	Behavioral DSM	17% peak reduction
Naccarelli et al. ³⁶	AI-based flexibility model	Comfort-driven demand response	Better grid alignment

Abbreviations: AI: Artificial intelligence; ANN: Artificial neural network; EWOA: Enhanced whale optimization algorithm; PAR: Peak-to-average ratio; PV: Photovoltaic; VOA: Virus optimization algorithm.^{bib33}

Table 4. Input parameters for photovoltaic (PV) sizing.

Parameter	Value/range	Parameter
PV panel size and rating	1.9 m ² , 0.325 kW per panel	PV panel size and rating
Usable roof area	250 m ²	Usable roof area
Max PV capacity	~ 43 kW	Max PV capacity
Capital cost (PV)	\$ 354.2/kW	Capital cost (PV)
Capital cost (inverter)	\$300/kW	Capital cost (inverter)
O&M cost (PV)	\$10/kW/year	O&M cost (PV)
O&M cost (inverter)	\$10/kW/year	O&M cost (inverter)
Replacement cost (PV)	\$ 354.2/kW	Replacement cost (PV)
Replacement cost (inverter)	\$300/kW	Replacement cost (inverter)
System lifetime	25 years	System lifetime

Abbreviation: O&M: Operation and maintenance.

3.1. Renewable energy sizing

The renewable capacity-planning problem minimizes the net present cost (NPC) while maximizing renewable utilization. NPC includes capital, operation and maintenance, replacement, grid-purchase, and export-revenue components, subject to rooftop, irradiance, and economic constraints (see **Table 4**).

3.1.1. HOMER pro-based optimization

The HOMER Pro-based optimization model was implemented as a standalone techno-economic algorithm to determine optimal PV capacity. It systematically simulated feasible PV-grid configurations and computed lifecycle cost via NPC minimization. The optimal configuration corresponds to the minimum NPC while satisfying technical

and spatial limits. Sensitivity analyses on discount rate, component cost, and irradiance validated design robustness.

As illustrated in **Figure 1**, HOMER Pro evaluates the techno-economic performance of different PV configurations by combining hourly simulation with cost optimization. The process begins with importing building load, meteorological, and economic data, ensuring consistent boundary conditions with the Q-Learning model. Design constraints such as roof area, component lifetimes, and inverter capacity are defined to limit feasible system sizes. HOMER Pro then runs iterative simulations across candidate PV capacities, each representing a distinct system configuration.

For every simulation, the software performs an hourly energy balance between PV generation, grid imports, and load demand, calculating

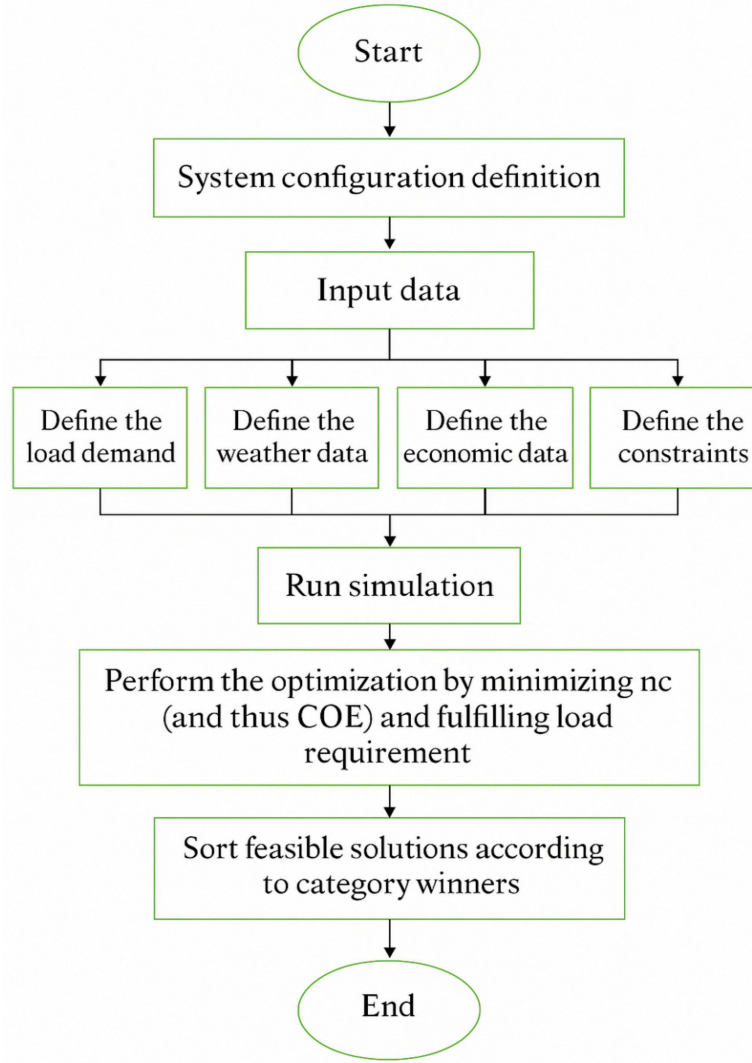


Figure 1. Process flowchart for sizing a renewable energy system using HOMER Pro (adapted from Yaouba et al. ⁴⁰; Copyright © 2022, The authors).

Abbreviations: COE: Cost of energy; NPC: Net present cost.

life-cycle economic indicators including NPC, levelized cost of energy, and renewable fraction. A sensitivity analysis explores the influence of uncertain parameters, such as discount rate or tariff variation, allowing the model to identify the most cost-effective and resilient configuration. Once convergence is achieved, the optimal design, typically characterized by minimal NPC and high renewable penetration, is selected as the reference for comparative analysis against the Q-Learning-based renewable energy system (RES) sizing results presented later in the study.

3.1.2. Reinforcement learning (Q-Learning)-based optimization

In parallel, a reinforcement-learning-based model using Q-Learning was developed on the same dataset to compare adaptive exploration with deterministic economic optimization. Each state

corresponds to a candidate PV capacity, while actions increase or decrease the capacity depending on the reward.

The reward function integrates economic, technical, and environmental terms:

$$R_t = w_1 * (-C_{NPC}) + w_2 * f_{REN} + w_3 * U_{roof} - w_4 * G_{grid} + w_5 * E_{export} \# (1)$$

where

- (1) C_{NPC} = system cost,
- (2) f_{REN} = renewable fraction,
- (3) U_{roof} = roof utilization,
- (4) G_{grid} = grid reliance,
- (5) E_{export} = exported PV energy, and
- (6) Weights ($w_1 \dots w_5$) are tuned by grid-search sensitivity analysis to balance economic and technical priorities.

For clarity and reproducibility, the Q-Learning formulation used in this study is explicitly defined as follows. In the PV sizing model, each state represents a discrete candidate PV capacity. The feasible range of 0–45 kW was discretized into steps of 0.2–0.4 kW to maintain a manageable table size while preserving sufficient resolution. Actions correspond to increasing, decreasing, or maintaining the PV capacity by one discretization step.

The reward function weights ($w_1 \dots w_5$) were selected through a grid-based sensitivity analysis in which 120 candidate weight combinations were evaluated to balance economic cost, renewable utilization, and grid dependence. Combinations that produced unstable training, excessive oscillation, or unrealistic PV sizing were discarded. The selected weight set provided stable learning and consistent convergence across repeated runs.

The Q -value update follows the Bellman equation:

$$Q(s, a) \leftarrow Q(s, a) + \alpha \left[r + \gamma \max_{a'} Q(s', a') - Q(s, a) \right] \quad (2)$$

with learning rate α and discount factor γ .

The resulting PV configurations achieved minimal NPC and high renewable fraction, supporting direct comparative analysis with the HOMER Pro-based model.

As shown in **Figure 2**, the RL-based RES sizing framework utilizes Q-Learning to determine the optimal PV capacity through adaptive value iteration rather than exhaustive search. The algorithm begins with the system inputs, hourly load, irradiance, temperature, tariff data, and component parameters, then defines discrete states representing possible PV capacity levels and actions corresponding to increasing, decreasing, or maintaining capacity. Learning parameters such as the learning rate (α), discount factor (γ), and exploration rate (ϵ) regulate how quickly the agent updates its knowledge and balances exploration with exploitation.

During each iteration, the agent selects an action using an ϵ -greedy policy and evaluates the resulting configuration by simulating energy and cost performance to obtain the NPC, renewable fraction, and grid reliance. A multi-objective reward function ($-\text{NPC} + \text{weighted renewable and utilization benefits} - \text{grid dependence penalty}$) quantifies the desirability of each state–action pair. The Q -values are updated according to the Bellman equation until convergence, indicating stable learning of the optimal PV capacity.

The final outcome, as illustrated in **Figure 2**, is an adaptive sizing strategy that minimizes life-cycle cost while maximizing renewable utilization

and rooftop efficiency. Compared to the static techno-economic optimization of HOMER Pro, the Q-Learning approach dynamically learns cost-effective configurations under changing tariffs and environmental conditions, providing a more flexible and intelligent sizing framework for building-level energy management systems.

3.2. Demand-side management

After sizing optimization, DSM scheduling minimizes electricity cost and maximizes PV self-consumption over a 24-hour horizon:

$C_{\text{DSM}} = \sum_t P_t E_t \# (3)$ where E_t is the shifted load at hour t and P_t is the ToU tariff. Only predefined flexible loads were subjected to shifting, maintaining comfort and operational limits. Both PSO and Q-Learning DSM models were implemented and executed independently under identical datasets to ensure a fair comparative evaluation.

3.2.1. Grid-only demand-side management optimization scenario

In this scenario, PSO and Q-Learning separately derive optimal schedules. Each PSO particle represents a daily load-shifting plan and iteratively updates velocity and position via inertia (ω), cognitive (c_1), and social (c_2) coefficients until convergence. Q-Learning defines states by hour, tariff, and load level, while actions represent “shift” or “maintain.” Rewards penalize peak-period consumption and encourage off-peak utilization. Both methods reduce the peak-to-average ratio and total cost relative to the baseline.

3.2.2. Grid + photovoltaic demand-side management optimization scenario

When PV is integrated, DSM coordination considers renewable availability. The Q-Learning state vector is expanded to include normalized PV generation, enabling adaptive policies that favor self-consumption. Rewards penalize grid imports during expensive hours and reinforce local PV use. The PSO model follows the same objective via swarm-based exploration. This coordinated approach enhances renewable fraction, reduces grid dependence, and improves cost efficiency compared with the grid-only configuration.

In the DSM model, each state is defined by the triplet (t, P, L) , representing the current hour, the ToU tariff level, and the normalized building load. When PV was integrated, normalized PV generation was added to the state vector. Actions represent whether a flexible load should be shifted or retained within its allowable time window, and

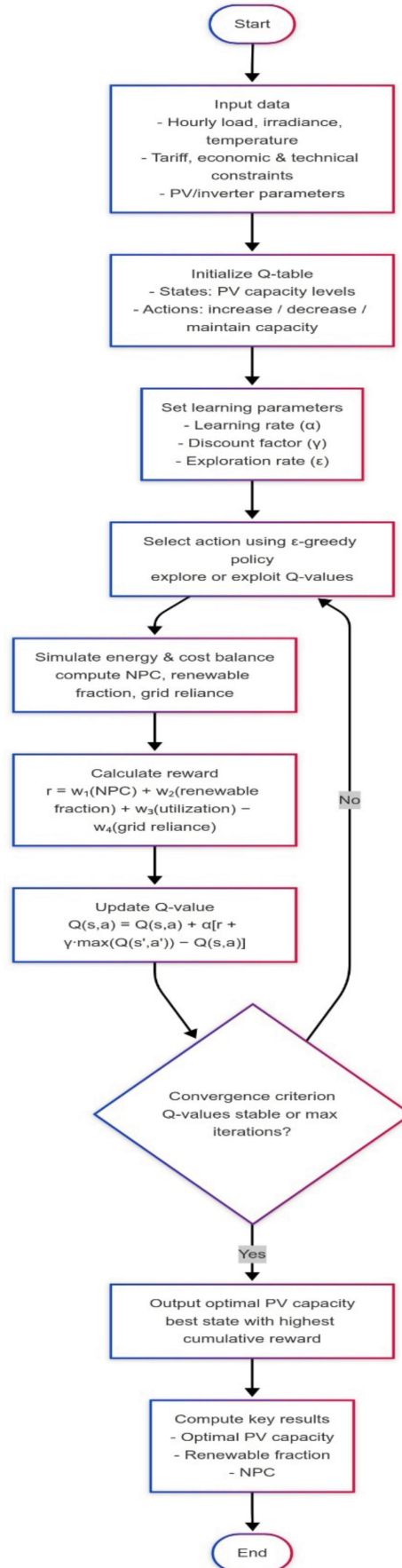


Figure 2. Flowchart of the Q-Learning-based renewable energy system (RES) sizing process. Abbreviations: NPC: Net present cost; PV: Photovoltaic.

all DSM actions preserved total daily energy while respecting predefined operational constraints.

Figure 3 illustrates the stepwise structure of the PSO algorithm developed for the DSM scheduling problem. The process begins with the initialization of input parameters, including the hourly load profile, ToU tariff, and, when applicable, the PV generation profile. Each particle in the swarm represents a candidate load-shifting schedule, and its fitness is evaluated based on the total daily energy cost as defined by the cost function $C_{DSM} = (\text{Shifted_LoadTariff} - \text{PV})$. Through iterative updates of velocity and position, particles are guided by individual ($pBest$) and global ($gBest$) best solutions to minimize cost. Load constraints such as shift limits, user comfort, and energy balance are continuously enforced during the optimization process. Convergence is achieved when the improvement between successive iterations falls below a predefined threshold, after which the optimal DSM schedule is produced along with key performance metrics, minimum daily cost, PV self-consumption, and grid reduction. This iterative structure allows PSO to balance exploration and exploitation, providing cost-efficient load scheduling across both grid-only and PV-integrated scenarios.

As shown in **Figure 4**, the Q-Learning framework replaces heuristic search with an adaptive decision-making process that learns optimal load-shifting behavior through repeated interaction with the environment. The agent begins with the system inputs—hourly demand, tariff structure, and PV availability—and defines discrete states representing each hour’s operating conditions, with actions determining whether a flexible load should be shifted or retained. Learning parameters, including the learning rate (α), discount factor (γ), and exploration rate (ϵ), control how new information influences the Q-table updates.

At each time step, the agent selects an action using an -greedy policy to balance exploration and exploitation. After executing the load-shifting decision, it observes a reward inversely proportional to the total electricity cost and grid dependence, thus encouraging self-consumption of available PV energy. The Q-values are iteratively updated using the Bellman equation to capture the expected future benefits of each decision. This loop continues until the convergence criterion is met, signifying that the agent has derived a stable optimal policy mapping every state to its most cost-effective action.

The final output, also depicted in **Figure 4**, provides a policy-based DSM schedule that minimizes daily energy cost, improves PV utilization, and reduces grid reliance compared to heuristic methods such as PSO. The RL approach, therefore, enables adaptive control capable of responding to real-time tariff and renewable variations within the BEMS.

The overall architecture comprises four interconnected layers (illustrated conceptually in **Figure 5**):

- (1) Input layer: imports building load profiles, tariffs, meteorological data, and technical constraints.
- (2) Design layer: executes renewable energy sizing using independent HOMER Pro (for techno-economic optimization) and Q-Learning models (for adaptive PV capacity exploration).
- (3) Optimization layer: conducts DSM scheduling using PSO and Q-Learning under both grid-only and grid + PV conditions.
- (4) Decision layer: outputs energy cost, renewable fraction, self-consumption, and optimal load schedules for performance comparison.

Together, these layers enable a unified and comparative analysis of deterministic and learning-based optimization strategies within a single intelligent BEMS framework.

3.3. Validation and verification

To assess computational feasibility, the runtime of each optimization method was evaluated using identical computing hardware. HOMER Pro completed the techno-economic sizing simulations in approximately 4–6 minutes per sensitivity sweep, while PSO-based DSM required 40–60 seconds per daily optimization, depending on swarm size. The Q-Learning PV sizing model required roughly 2–3 minutes for 300–400 training episodes, and the DSM agent converged in 20–30 seconds. Although RL incurs higher offline training costs, the learned policy can be reused for operation without retraining, making it suitable for design studies and periodic re-optimization.

While full real-world stochasticity—including occupancy variation, sensor uncertainty, and PV intermittency forecasting errors—was not modeled, the conducted sensitivity tests on irradiance, tariffs, and discount rate provide a baseline robustness assessment within a simulation-level study. Extending the framework to incorporate richer uncertainty modeling is an important avenue for future work.

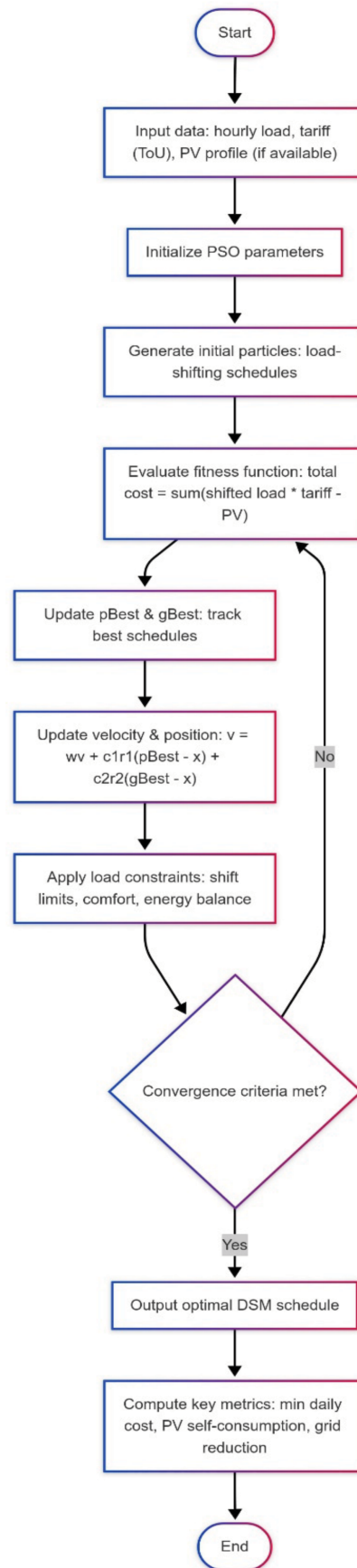


Figure 3. Flowchart of the particle swarm optimization algorithm (PSO) for the demand-side management (DSM) problem under both grid-only and grid + photovoltaic (PV) configurations. Abbreviation: ToU: Time-of-use.

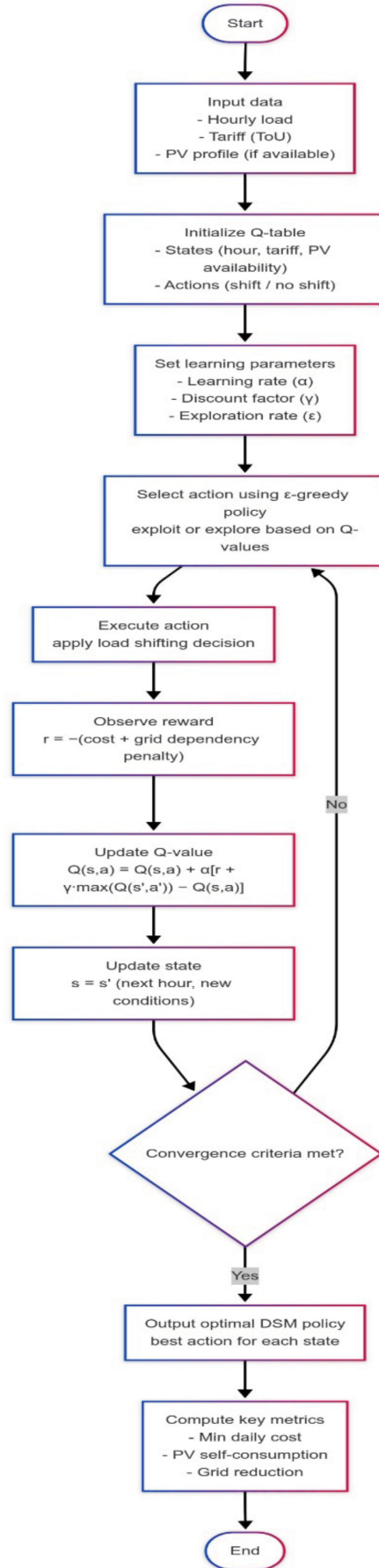


Figure 4. Flowchart of the Q-Learning algorithm applied to demand-side management (DSM) optimization for grid-only and grid + photovoltaic (PV) configurations.
Abbreviation: ToU: Time-of-use.

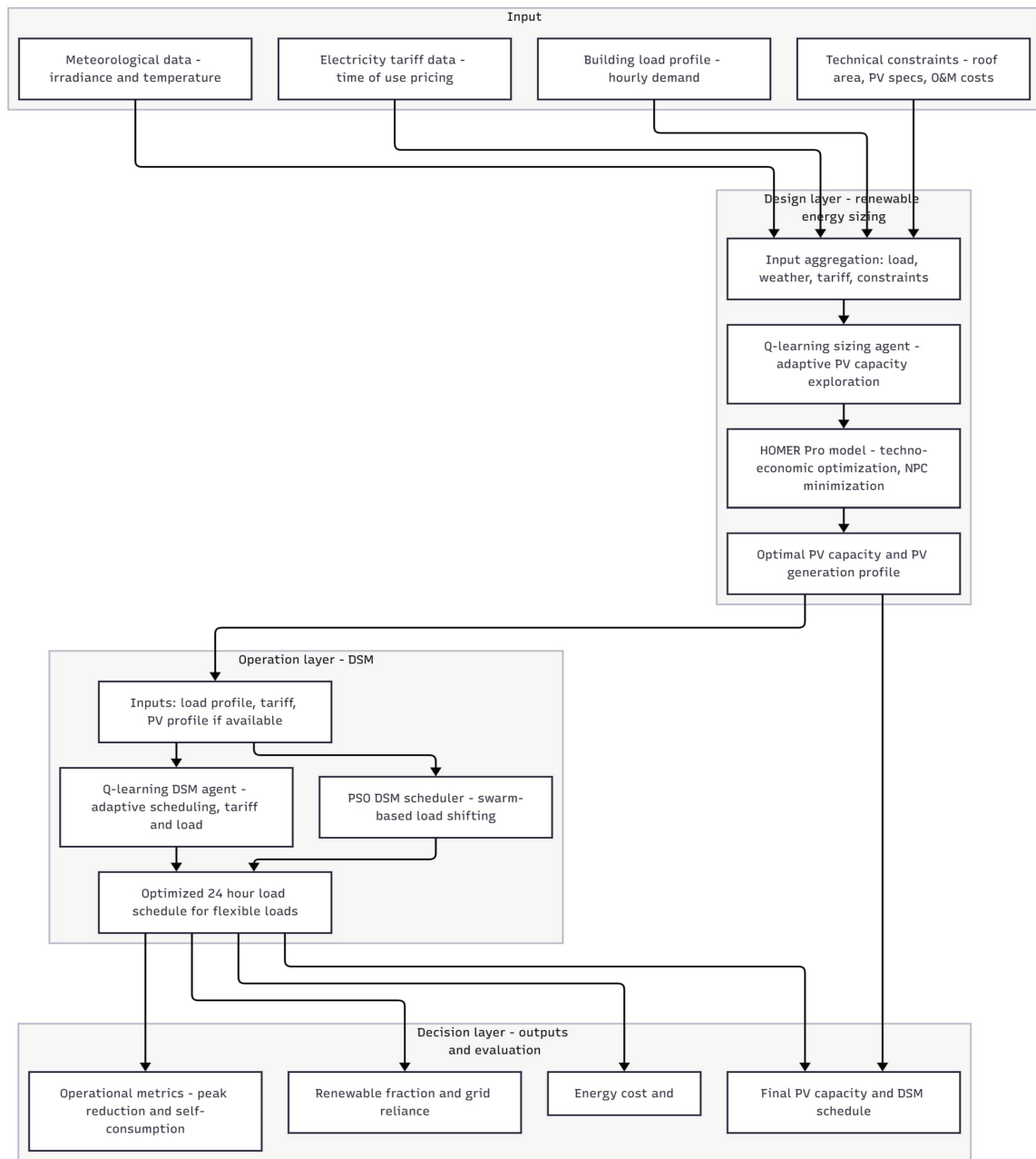


Figure 5. Proposed artificial intelligence-driven building energy management system architecture. Abbreviations: DSM: Demand-side management; NPC: Net present cost; O&M: Operation and management; PSO: Particle swarm optimization; PV: Photovoltaic.

To ensure the accuracy and reliability of the proposed AI-driven BEMS framework, several validation procedures were performed. First, the Q-Learning models used for renewable energy sizing and DSM were evaluated through repeated simulation runs to confirm consistent behavior and stable policy generation. In all cases, the learned Q-tables produced repeatable sizing and scheduling outcomes that aligned with the expected performance trends of the annual dataset, confirming stable convergence under the selected learning parameters.

Second, model output consistency was assessed through cross-comparison with deterministic methods. The optimal PV capacity identified by the Q-Learning sizing model—approximately 42.2 kW—closely matched the HOMER Pro result, demonstrating that the learning-based approach can reliably reproduce a techno-economic optimum. Likewise, the DSM schedules generated by Q-Learning showed greater load-shifting capability and slightly higher cost reductions than those produced by PSO, in agreement with the detailed seasonal results presented in this study.

Sensitivity tests examining discount-rate variation (7–10%), irradiance fluctuations ($\pm 10\%$), and tariff adjustments indicated that both the Q-Learning and deterministic models retained stable performance across parameter changes. These tests confirmed that the optimization outputs are robust within realistic uncertainty bounds. As this study is simulation-based, practical deployment would require additional considerations—such as sensor accuracy, occupant variability, and communication constraints—which lie outside the scope of this work.

The proposed framework integrates renewable energy sizing and adaptive DSM within a unified AI-based BEMS architecture. The design layer applied HOMER Pro and Q-Learning for PV capacity optimization, while the operational layer used PSO and Q-Learning for DSM scheduling under both grid-only and grid + PV conditions. This modular and reproducible structure supported direct comparison between deterministic and learning-based optimization techniques. Overall, the framework unified RES sizing and DSM control within a single intelligent BEMS, offering a scalable and flexible approach that enhances coordination and simulation-based performance.

4. Results and discussion

This section presents and analyzes the outcomes of the proposed AI-driven BEMS integrating Q-Learning-based optimization for both renewable energy sizing and DSM. The Q-Learning framework was benchmarked against HOMER Pro for capacity planning and PSO for load scheduling. All models shared identical hourly inputs, load demand from the DOE mid-rise apartment reference building, meteorological data from NASA POWER, and real Miami ToU tariffs, to ensure fair and reproducible comparison under grid-only and grid + PV configurations.

4.1. Model verification and validation

Model verification and validation were performed to ensure numerical correctness, physical plausibility, and consistent performance. Energy balance was satisfied for all configurations (mismatch $< 1\%$), confirming the physical validity of the annual simulations. The Q-Learning agents used for both sizing and DSM produced stable and repeatable outcomes across multiple runs, indicating reliable policy convergence under the selected learning parameters. Sensitivity tests performed on key inputs—including $\pm 10\%$ irradiance, $\pm 5\%$ tariff variation, and 7–10% discount-rate changes—resulted in less than 3% deviation

in total cost, demonstrating robustness of the optimization outputs. These checks confirm that the proposed framework maintains consistent physical and economic integrity across all objectives.

4.2. Renewable energy sizing

4.2.1. HOMER Pro

The deterministic HOMER Pro model established a techno-economic baseline for PV sizing. The optimal configuration consisted of a 42.0 kW PV array coupled with a 29.8 kW inverter, fully meeting the annual load with no unserved energy. Annual PV generation reached 64,579 kW h, while grid purchases totaled 265,470 kW h and grid exports 1,193 kW h, resulting in a renewable fraction of 18.6%. The corresponding NPC over the 25-year project lifetime was US\$566,522. The comparative results between HOMER Pro and the Q-learning optimization are summarized in **Table 5**, demonstrating strong alignment across the main techno-economic indicators. HOMER Pro thus delivers a technically feasible and economically consistent configuration under the specified load, tariff, and resource assumptions. However, its optimization remains largely static: inverter sizing and dispatch follow deterministic rules, limiting responsiveness to hourly tariff changes and PV variability. As a result, the HOMER-based solution provides a robust baseline but cannot fully exploit dynamic opportunities for enhanced self-consumption, export, or cost reduction.

4.2.2. Reinforcement learning (Q-Learning)

Using identical datasets, the Q-Learning model converged to a PV capacity of 42.2 kW together with a 30 kW inverter, closely matching the HOMER Pro configuration while remaining within rooftop and inverter constraints. This adaptive configuration preserved full load reliability and achieved nearly identical technical performance to the deterministic model, with only marginal differences in hourly energy flows. Performance outcomes were very similar to those of HOMER Pro:

- (1) Grid imports: 265,088 kW h ($\approx 0.14\%$ lower)
- (2) Grid exports: 1,193.4 kW h ($\approx 0.03\%$ higher)
- (3) Renewable fraction: 19.2% ($\approx 3.1\%$ increase)
- (4) NPC: US\$556,063 ($\approx -1.85\%$ difference)

These results indicate that the RL-based sizing method can independently reproduce a near-identical PV-grid configuration and deliver a slightly lower lifecycle cost.

Three factors explain the Q-Learning performance:

- (1) Operational flexibility: The 30 kW inverter was automatically selected by the agent to balance PV utilization, grid interaction, and roof area limits with minimal oversizing.
- (2) Tariff-aware learning: The reward function integrated hourly electricity price signals, guiding the agent toward configurations that minimize long-term grid-purchase cost.
- (3) Integrated design–operation evaluation: The RL agent evaluated each PV–inverter pair using a full-year techno-economic simulation, ensuring that only economically robust configurations received positive reinforcement.

Although the Q-Learning configuration differed only slightly from the HOMER-derived design, the small reduction in grid purchases and nearly identical export behavior produced a modest but measurable reduction in NPC. Sensitivity tests under $\pm 10\%$ irradiance and $\pm 5\%$ tariff variations produced $< 3\%$ deviation in total cost, confirming the solution's robustness. Hourly energy-balance verification (mismatch $< 1\%$) and the close alignment with HOMER Pro metrics confirmed that the RL-based system is both physically consistent and economically sound.

4.3. Demand-side management

The DSM analysis compared Q-Learning and PSO under identical winter and summer load profiles and the same ToU tariff structure. Flexible loads were shifted within operational constraints to minimize daily cost while preserving total energy consumption.

4.3.1. Grid-only scenario

Without PV availability, both algorithms relied entirely on tariff signals to reschedule flexible loads:

- (1) Q-Learning:
 - (a) Winter: US\$97.58 \rightarrow US\$90.18 (-7.58%) with 128.68 kW h shifted (19.96%).
 - (b) Summer: US\$154.68 \rightarrow US\$141.89 (-8.27%) with 222.49 kW h shifted (22.34%).
- (2) PSO:
 - (a) Winter: US\$97.58 \rightarrow US\$94.38 (-3.28%) with 98.14 kW h shifted (15.22%).

- (b) Summer: US\$154.68 \rightarrow US\$150.25 (-2.86%) with 151.73 kW h shifted (15.23%).

These results show that Q-Learning consistently shifted a larger share of flexible loads and achieved greater cost reductions in both seasons. PSO responded more conservatively to tariff variations, whereas Q-Learning responded to hourly price signals more effectively, producing stronger peak-shaving and enhanced off-peak utilization (**Figures 6 and 7**).

Q-Learning consistently achieved larger load shifts and greater cost reductions than PSO by responding more effectively to hourly tariff variations. While both algorithms used identical tariff inputs, Q-Learning demonstrated a stronger ability to relocate flexible loads from high-price periods to cheaper off-peak intervals, producing noticeably higher savings in both winter and summer cases. PSO exhibited a more conservative response with smaller shifts and reduced savings, reflecting its limited sensitivity to rapid changes in tariff patterns. In all scenarios, total daily energy was preserved, and operational constraints were satisfied, confirming the physical feasibility of the DSM schedules generated.

4.3.2. Grid + photovoltaic scenario

When PV generation was available, both algorithms coordinated DSM with the solar production window to reduce grid dependence.

- (1) Q-Learning grid + PV:
 - (a) Winter: US\$97.58 \rightarrow US\$63.32 (-35.14%) with 15.76 kW h shifted (24.67%).
 - (b) Summer: US\$154.68 \rightarrow US\$113.04 (-26.89%) with 23.94 kW h shifted (23.93%).
- (2) PSO grid + PV:
 - (a) Winter: US\$97.58 \rightarrow US\$64.70 (-33.68%) with 13.06 kW h shifted (20.48%).
 - (b) Summer: US\$154.68 \rightarrow US\$119.16 (-22.98%) with 13.59 kW h shifted (13.80%).

These results demonstrate that PV availability substantially improved DSM effectiveness, and Q-Learning consistently achieved higher cost reductions by aligning flexible loads more precisely with daytime solar generation.

Photovoltaic availability significantly enhanced DSM performance by allowing flexible loads to be shifted into periods with daytime solar generation. In this setting, Q-Learning aligned load schedules with PV production more effectively than PSO, resulting in slightly higher

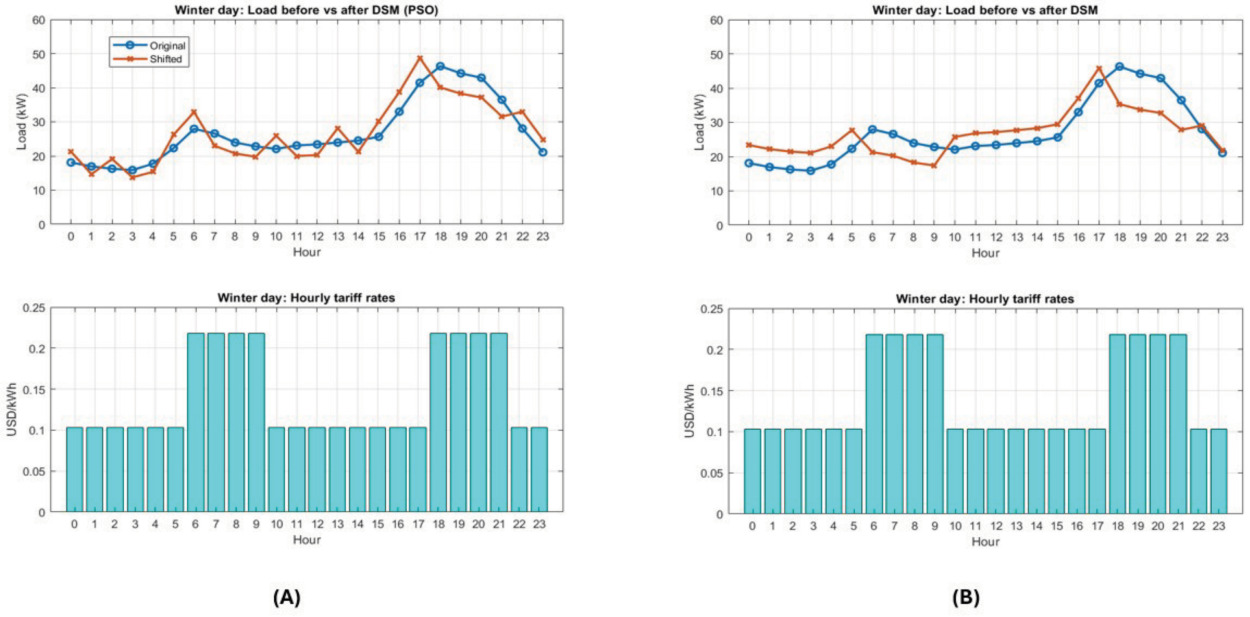


Figure 6. Winter day load shifting under grid-only demand-side management (DSM): (A) Particle particle swarm optimization (PSO); (B) Q-Learning.

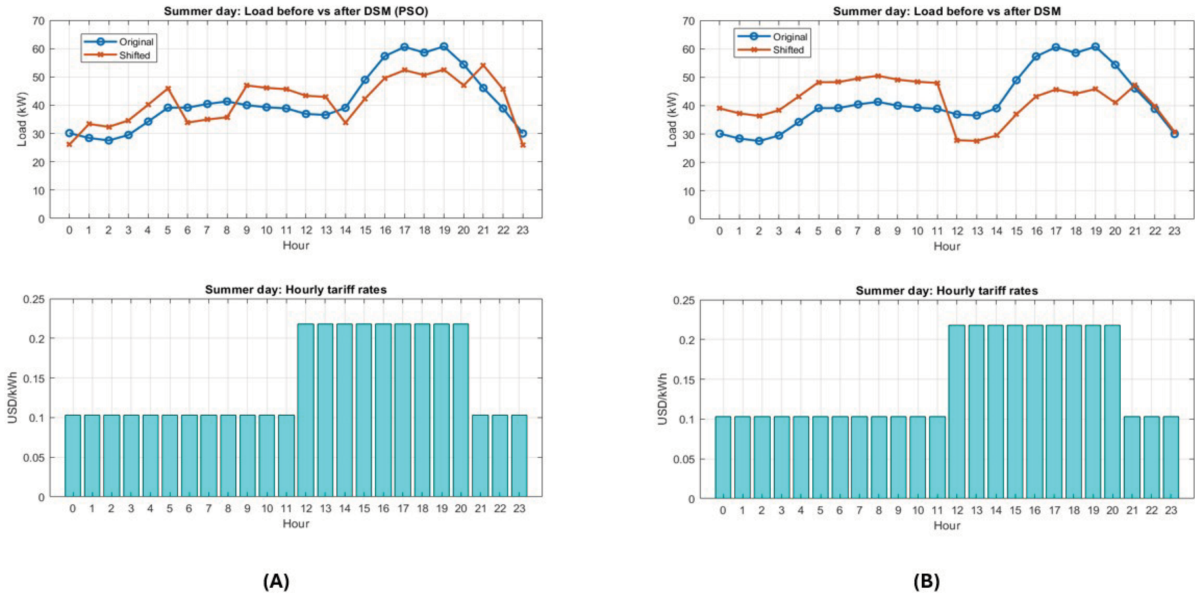


Figure 7. Summer day load shifting under grid-only demand-side management (DSM): (A) Particle particle swarm optimization (PSO); (B) Q-Learning.

cost reductions in both winter and summer cases. While PSO benefitted from PV generation, its shifting strategy was more conservative and less precisely synchronized with the solar window. Q-Learning, by contrast, rescheduled a larger share of flexible demand into PV hours, improving day-time self-consumption and reducing reliance on the grid during high-tariff periods.

The graphical results also highlight clear seasonal differences in algorithm performance. During winter, limited solar availability reduced the

opportunity for midday load shifting, causing both PSO and Q-Learning to rely more heavily on tariff signals. In contrast, the summer plots show pronounced midday load relocation due to higher PV output. Q-Learning demonstrated sharper alignment between load demand and PV generation, particularly in hours 10–15, producing higher self-consumption and deeper reductions in peak-period grid imports. These graphical observations reinforce the numerical findings reported in **Tables 5-7**.

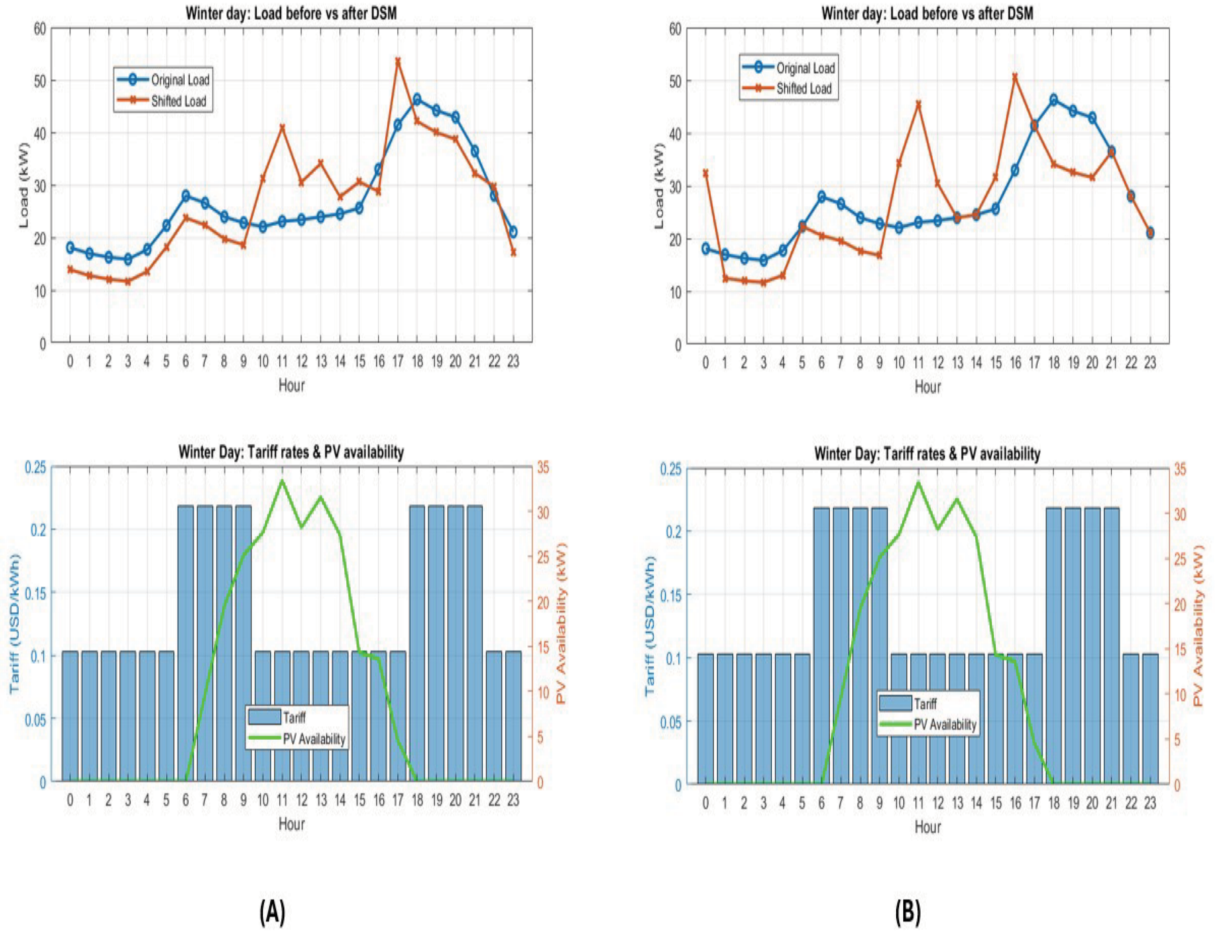


Figure 8. Winter day demand-side management (DSM) with photovoltaic (PV) integration: (A) Particle particle swarm optimization (PSO); (B) Q-Learning.

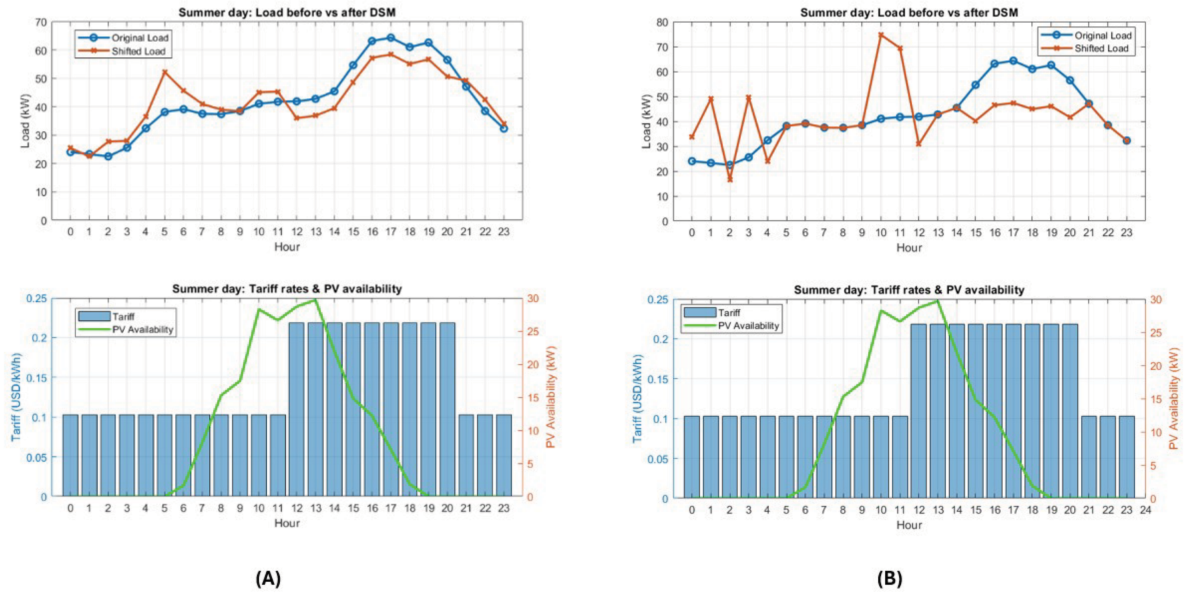


Figure 9. Summer day demand-side management (DSM) with photovoltaic (PV) integration: (A) Particle particle swarm optimization (PSO); (B) Q-Learning.

Table 5. Optimal renewable energy system configuration—HOMER Pro versus Q-Learning.

Parameter	Homer Pro	Q-Learning	% difference	Notes
PV capacity (kW)	42.0	42.2	+0.48%	Identical within rounding
Inverter capacity (kW)	29.8	30.0	+0.67%	RL independently matches HOMER's selection
Annual PV generation (kW h)	64,579	62,426	−3.33%	Minor differences due to hourly irradiance modeling
Grid energy purchased (kW h)	265,470	265,088	−0.14%	Excellent alignment
Grid energy sold (kW h)	1,193	1,193.4	+0.03%	Nearly identical
Renewable fraction (%)	18.6%	19.2%	+3.1%	Very close

Abbreviations: PV: Photovoltaic RL: Reinforcement learning.

Table 6. Economic performance—Q-Learning versus HOMER Pro.

Economic metric	HOMER Pro	Q-Learning	% difference	Interpretation
NPC (USD)	566,522	556,063	−1.85%	RL achieves slightly lower lifecycle costs
Initial Capital (USD)	14,876	14,947	+0.5%	Minor difference due to PV rounding
Annual operating cost (USD/yr)	Similar	Similar	–	Near-identical grid interaction patterns
Renewable fraction (%)	18.6%	19.2%	+3.1%	Small increase in annual PV contribution

Abbreviations: NPC: Net present cost; PV: Photovoltaic; RL: Reinforcement learning; USD: United States dollars.

Table 7. Daily energy cost comparison for demand-side management (DSM) strategies.

DSM strategy	Winter cost (US\$)	Summer cost (US\$)	% reduction (winter)	% reduction (summer)
Without DSM (baseline)	97.58	154.68	0	0
PSO (grid only)	94.38	150.25	3.28	2.86
Q-Learning (grid only)	90.18	141.89	7.58	8.27
PSO (grid + PV)	64.70	119.16	33.68	22.98
Q-Learning (grid + PV)	63.32	113.04	35.14	26.89

Abbreviations: PSO: Particle swarm optimization; PV: Photovoltaic.

Across all PV-integrated scenarios, both algorithms preserved total daily energy and respected operational constraints, confirming the feasibility of the resulting schedules. The comparative evaluation presented here shows that Q-Learning maintained a consistent performance advantage over PSO by responding more adaptively to the combined effects of PV availability and tariff variations. These findings highlight the potential of

learning-based DSM methods to improve cost efficiency and renewable-energy utilization within BEMS (**Figures 8 and 9**).

5. Conclusion

This study presents an integrated AI-driven BEMS that combines RES sizing and DSM using RL (Q-Learning) and evaluates its performance against deterministic approaches such as

HOMER Pro and PSO. The proposed framework enabled a unified assessment of learning-based and rule-based optimization techniques under both grid-only and PV-integrated operating conditions.

The study is subject to several limitations. The DSM model used simplified assumptions that do not fully capture occupant behavior, appliance cycling, or thermal comfort constraints. The RL models did not incorporate forecasting errors or stochastic load variations, and DRL approaches were not explored. Future work will extend the framework with uncertainty-aware RL, DRL architectures such as deep deterministic policy gradient and proximal policy optimization, real-time occupancy integration, and multi-building coordination to support more realistic deployment and improve generalizability.

The results show that the Q-Learning model achieved a PV-inverter configuration that closely matched the techno-economic optimum produced by HOMER Pro, with a slightly lower NPC (−1.85%) and a marginally higher renewable fraction (+3.1%). For DSM, Q-Learning consistently outperformed PSO by shifting a larger portion of flexible loads and achieving greater cost reductions across both winter and summer scenarios. Under grid-only conditions, Q-Learning reduced daily costs by 7.58% in winter and 8.27% in summer. With PV integration, savings increased to 35.14% in winter and 26.89% in summer, modestly exceeding those obtained with PSO.

These findings confirm that RL can reproduce and modestly improve the outcomes of conventional optimization tools by adapting more effectively to tariff variations and renewable availability. Both Q-Learning and PSO maintained energy balance and respected operational constraints, demonstrating the feasibility of the generated schedules within a realistic BEMS environment.

Overall, this research highlights the practical value of RL for intelligent energy management. By offering a flexible, data-driven alternative to static optimization tools, Q-Learning enhances DSM performance and provides a competitive approach for RES planning. Future work may extend the framework to more detailed comfort modeling, multi-building coordination, and integration with evolving tariff and market structures.

Acknowledgments

None.

Funding

None.

Conflict of interest

The authors declare that they have no competing interests.

Author contributions

Conceptualization: Karim ElNaggar

Formal analysis: Karim ElNaggar

Investigation: Karim ElNaggar

Methodology: All authors

Supervision: Rana Maher, Motaz Amer, Amany El-Zonkoly

Validation: Rana Maher, Motaz Amer, Amany El-Zonkoly

Writing—original draft: Karim ElNaggar

Writing—review & editing: Rana Maher, Motaz Amer, Amany El-Zonkoly

Availability of data

The datasets generated and/or analyzed during the current study are available from the corresponding author upon reasonable request.

AI tools statement

The authors confirm that QuillBot was used solely for language refinement and writing enhancements. No AI tools were used for data analysis, methodological development, result generation, or interpretation of findings.


References

- Correia S, Matos-Carvalho JP, Kim C, et al. Real-Time time AI-Based based power demand forecasting for peak shaving and consumption reduction using vehicle-to-grid and reused energy storage systems: a case study at a business center on Jeju Island. *Appl. Sci. (Basel)* 2025;15(1):3050, Vol 15, Page 3050 15:3050. <https://doi.org/10.3390/APP15063050>
- Kwon K, Lee S, Kim S. AI-based home energy management system considering energy efficiency and resident satisfaction. *IEEE Internet Things J.* 2022;9(2):1608-1621. <https://doi.org/10.1109/JIOT.2021.3104830>
- Ali ANF, Sulaima MF, Razak IAWA, et al. Artificial intelligence application in demand response: advantages, issues, status, and challenges. *IEEE Access.* 2023;11:16907-16922. <https://doi.org/10.1109/ACCESS.2023.3237737>


4. Lin Y, Tang J, Guo J, et al. Advancing AI-enabled techniques in energy system modeling: a review of data-driven, mechanism-driven, and hybrid modeling approaches. *Energies (Basel)*. 2025;18:845. <https://doi.org/10.3390/en18040845>
5. Yu S, Liu X, Li R, et al. Demand side management full season optimal operation potential analysis for coupled hybrid photovoltaic/thermal, heat pump, and thermal energy storage systems. *J Energy Storage*. 2024; 80:110375. <https://doi.org/10.1016/J.EST.2023.110375>
6. Liu Z, Zhang X, Sun Y, Zhou Y. Advanced controls on energy reliability, flexibility and occupant-centric control for smart and energy-efficient buildings. *Energy Build.* 2023;297:113436. <https://doi.org/10.1016/J.ENBUILD.2023.113436>
7. Li D, Qi Z, Zhou Y, Elchalakani M. Machine learning applications in building energy systems: review and prospects. *Buildings*. 2025;648(15):648. <https://doi.org/10.3390/BUILDINGS15040648>
8. Agostinelli S, Cumo F, Guidi G, Tomazzoli C. Cyber-physical systems improving building energy management: digital twin and artificial intelligence. *Energies*. 2021;14:2338. <https://doi.org/10.3390/EN14082338>
9. Mariano-Hernández D, Hernández-Callejo L, Zorita-Lamadrid A, et al. A review of strategies for building energy management system: Model model predictive control, demand side management, optimization, and fault detect & diagnosis. *J Build Eng*. 2021;33:101692. <https://doi.org/10.1016/J.JOBE.2020.101692>
10. Behzadi A, Thorin E, Duwig C, Sadrizadeh S. Supply-demand side management of a building energy system driven by solar and biomass in Stockholm: A a smart integration with minimal cost and emission. *Energy Convers Manag.* 2023;292:117420. <https://doi.org/10.1016/J.ENCONMAN.2023.117420>
11. Shen R, Zhong S, Wen X, et al. Multi-agent deep reinforcement learning optimization framework for building energy system with renewable energy. *Appl Energy*. 2022;312:118724. <https://doi.org/10.1016/J.APENERGY.2022.118724>
12. Ramesh S, N SB, Sathyavarapu SJ, et al. Comparative analysis of Q-learning, SARSA, and deep Q-network for microgrid energy management. *Sci Rep*. 2025;15:1-11. <https://doi.org/10.1038/S41598-024-83625-8;SUBJMETA>
13. Vázquez-Canteli JR, Nagy Z. Reinforcement learning for demand response: A a review of algorithms and modeling techniques. *Appl Energy*. 2019;235:1072-1089. <https://doi.org/10.1016/J.APENERGY.2018.11.002>
14. Menos-aikateriniadis C, Lamprinos I, Georgilakis PS. Particle swarm optimization in residential demand-side management: a review on scheduling and control algorithms for demand response provision. *Energies*. 2022;15:2211 15:2211. <https://doi.org/10.3390/EN15062211>
15. Paul K, Jyothi B, Kumar RS, et al. Optimizing sustainable energy management in grid connected microgrids using quantum particle swarm optimization for cost and emission reduction. *Sci Rep*. 2025;15:1-20. <https://doi.org/10.1038/S41598-025-90040-0;SUBJMETA>
16. Latoń D, Grela J, Ozadowicz A. Applications of deep reinforcement learning for home energy management systems: a review. *Energies*. 2024;17:6420. <https://doi.org/10.3390/EN17246420>
17. Liu Y, Zhang D, Gooi HB. Optimization strategy based on deep reinforcement learning for home energy management. *CSEE Journal of Power and Energy Syst*. 2020;6:572-582. <https://doi.org/10.17775/CSEEJPES.2019.02890>
18. Ojand K, Dagdougui H. (2022) Q-Learning-based model predictive control for energy management in residential aggregator. *IEEE Trans Autom Sci Eng*. 2022;19:70-81. <https://doi.org/10.1109/TASE.2021.3091334>
19. Gbadega PA, Sun Y. A hybrid constrained particle swarm optimization-model predictive control (CPSO-MPC) algorithm for storage energy management optimization problem in micro-grid. *Energy Rep*. 2022;8:692-708. <https://doi.org/10.1016/J.EGYR.2022.10.035>
20. Liu J, Wang M, Peng J, et al. Techno-economic design optimization of hybrid renewable energy applications for high-rise residential buildings. *Energy Convers Manag.* 2020;213:112868. <https://doi.org/10.1016/J.ENCONMAN.2020.112868>
21. Das BK, Alotaibi MA, Das P, et al. Feasibility and techno-economic analysis of stand-alone and grid-connected PV/Wind/Diesel/Batt hybrid energy system: a a case study. *ESRnergy Strategy Reviews*. 2021;37:100673. <https://doi.org/10.1016/J.ESR.2021.100673>
22. Emrani A, Berrada A, Arechkik A, Bakhouya M. Improved techno-economic optimization of an off-grid hybrid solar/wind/gravity energy storage system based on performance indicators. *J Energy Storage*. 2022;49:104163. <https://doi.org/10.1016/J.EST.2022.104163>
23. Wankouo Ngouleu CA, Koholé YW, Fohagui FCV, Tchuen G. Optimum design and scheduling strategy of an off-grid hybrid photovoltaic-wind-diesel system with an electrochemical, mechanical, chemical and thermal energy storage systems: A a comparative scrutiny. *Appl Energy*. 2025;377:124646. <https://doi.org/10.1016/J.APENERGY.2024.124646>

24. Chegari B, Tabaa M, Simeu E, El Ganaoui M. Optimal energy management of a hybrid system composed of PV, wind turbine, pumped hydropower storage, and battery storage to achieve a complete energy self-sufficiency in residential buildings. *IEEE Access*. 2024; 12:126624-126639. <https://doi.org/10.1109/ACCESS.2024.3454149>
25. Medghalchi Z, Taylan O. A novel hybrid optimization framework for sizing renewable energy systems integrated with energy storage systems with solar photovoltaics, wind, battery and electrolyzer-fuel cell. *Energy Convers Manag*. 2023;294:117594. <https://doi.org/10.1016/J.ENCONMAN.2023.117594>
26. Jahanbin A, Abdolmaleki L, Berardi U. Techno-economic feasibility of integrating hybrid battery-hydrogen energy storage system into an academic building. *Energy Convers Manag*. 2024;309:118445. <https://doi.org/10.1016/J.ENCONMAN.2024.118445>
27. Abbas AK, Ayop R, Tan CW, et al. Advanced energy-management and sizing techniques for renewable microgrids with electric-vehicle integration: a review. *Res Eng*. 2025;27:106252. <https://doi.org/10.1016/J.RINENG.2025.106252>
28. Iqbal S, Sarfraz M, Ayyub M, et al. (2021) A comprehensive review on residential demand side management strategies in smart grid environment. *Sustainability*. 2021;13:7170. <https://doi.org/10.3390/SU13137170>
29. Hemanth GR, Charles Raja S, Jeslin Drusila Nesamalar J, Senthil Kumar J. Cost effective energy consumption in a residential building by implementing demand side management in the presence of different classes of power loads. *Adv Buil Energy Res*. 2022;16:145-170. <https://doi.org/10.1080/17512549.2020.1752799>
30. Farrokhifar M, Bahmani H, Faridpak B, et al. Model predictive control for demand side management in buildings: a survey. *Sustain Cities Soc*. 2021;75:103381. <https://doi.org/10.1016/J.SCS.2021.103381>
31. Tepe İF, Irmak E. Optimizing real-time demand response in smart homes through fuzzy-based energy management and control system. *Electrical Eng.ineering* 2025;107:2121—2145. <https://doi.org/10.1007/S00202-024-02613-3/TABLES/8>
32. Jasim AM, Jasim BH, Flah A, et al. A new optimized demand management system for smart grid-based residential buildings adopting renewable and storage energies. *Energy Rep*. 2023;9:4018-4035. <https://doi.org/10.1016/J.EGYR.2023.03.038>
33. Fernández Bandera C, Bastos Porsani G, Fernández-Vigil Iglesias M. A demand side management approach to increase self-consumption in buildings. *Buil Simul*. 2022; 16:2 16:317-335. <https://doi.org/10.1007/S12273-022-0933-9>
34. Philipo GH, Kakande JN, Krauter S. (2022) Neural network-based demand-side management in a stand-alone solar pv-battery microgrid using load-shifting and peak-clipping. *Energies*. 2022;15:5215. <https://doi.org/10.3390/EN15145215>
35. Doma A, Padsala R, Ouf MM, Eicker U. (2024) Bottom-up framework for modelling occupancy-based demand-side management strategies in a mixed-use district. *Appl Energy*. 2024;375:124081. <https://doi.org/10.1016/J.APENERGY.2024.124081>
36. Naccarelli R, Serroni S, Casaccia S, et al. Methodological approach for optimizing demand response in building energy management through AI-enhanced comfort-based flexibility models. In: 2024 9th International Conference on Smart and Sustainable Technologies, (SpliTech, 2024). <https://doi.org/10.23919/SPLITECH61897.2024.10612382>
37. Archive Reference Buildings by Building Type: Midrise Apartment | Department of Energy; 2025. <https://www.energy.gov/eere/articles/archive-reference-buildings-building-type-midrise-apartment>. Accessed 27 Sep 2025
38. NASA. NASA Prediction Of Worldwide Energy Resource (POWER); 2020. <https://Power.Larc.Nasa.Gov/Data-Access-Viewer/>
39. Florida Power & Light (FPL) Time-of-Use (TOU) ratesRates; 2025.<https://www.fpl.com/rates/time-of-use.html>. Accessed 28 Jun 2025
40. Yaouba, Zieba Falama R, Ngangoum Welaji F, et al. Optimal decision-making on hybrid off-grid 754181945energy754181945CECE754181945-941841423AU: Please provide volume number in Ref. 40. systems for rural and remote areas electrification in the Northern Cameroon. *J Electr Comput Eng*. 2022;1-14. <https://doi.org/10.1155/2022/5316520>

Karim ElNaggar is a Teaching Assistant and M.Sc. candidate in Electrical and Control Engineering at the Arab Academy for Science, Technology and Maritime Transport (AASTMT), Alexandria, Egypt. His research focuses on renewable energy systems, power electronics, and intelligent control of electrical systems, with an emphasis on reinforcement learning-based optimization for hybrid renewable energy and propulsion systems. He instructs courses in power electronics and marine electrical technology. Beyond academia, he is an active member of the IEEE Systems and Nanotechnology Councils and serves as a technical judge for national robotics competitions. His interests include sustainable maritime technologies and smart energy management.


 <https://orcid.org/0009-0006-0824-0430>

Rana Maher is an Associate Professor of Electrical and Control Engineering at the Arab Academy for Science, Technology & Maritime Transport (AASTMT) in Alexandria, Egypt. She holds a Ph.D. in Energy Management from Aix-Marseille University. Her research expertise is concentrated in renewable energy, smart grids, and power systems. Dr. Maher's published work includes studies on energy management for hybrid renewable energy sources and the development of smart traffic management systems utilizing IoT and PV power. She is a dedicated faculty member contributing to the advancement of electrical engineering and sustainable energy solutions.


 <https://orcid.org/0000-0002-2840-7975>

Motaz Amer is an Associate Professor at the Arab Academy for Science, Technology, and Maritime Transport (AASTMT), affiliated with the Basic and Applied Sciences Institute. He earned his Ph.D. in Energy Management from Aix-Marseille University (2015), following M.Sc. and B.Sc. degrees in Electrical Engineering from AASTMT. His primary research

interests are in Energy Management, Environmental Engineering, and Electrical Engineering. Dr. Amer's work has contributed to the fields of smart home energy management systems, power consumption optimization, and the optimal placement and sizing of distributed generation units.

 <https://orcid.org/0000-0002-0432-7444>

Amany El-Zonkoly is a Professor in the Department of Electrical & Control Engineering at the Arab Academy for Science, Technology & Maritime Transport (AASTMT). She completed her M.Sc. at Alexandria University in 1999 and her Ph.D. at Tanta University in 2003. Professor El-Zonkoly's research is focused on power system planning and operation, distributed generation, and power system optimization. She is a highly-cited researcher in her field, with notable contributions to the optimal allocation and sizing of plug-in hybrid electric vehicle (PHEV) parking lots within distribution systems.

 <https://orcid.org/0000-0002-6625-2601>

An International Journal of Optimization and Control: Theories & Applications
(<https://accscience.com/journal/ijocta>)



This work is licensed under a Creative Commons Attribution 4.0 International License. The authors retain ownership of the copyright for their article, but they allow anyone to download, reuse, reprint, modify, distribute, and/or copy articles in IJOCTA, so long as the original authors and source are credited. To see the complete license contents, please visit <http://creativecommons.org/licenses/by/4.0/>.